WHOLE EXOME SEQUENCING IDENTIFIES CANDIDATE GENES FOR AUTOSOMAL DOMINANT MESOMANDIBULAR FIBRO-OSSEOUS DYSPLASIA (ADMFOD), A SELF-RESOLVING INHERITED FIBRO-OSSEOUS LESION OF THE JAWS, UNRELATED TO FIBROUS DYSPLASIA

A THESIS
SUBMITTED TO THE FACULTY OF
UNIVERSITY OF MINNESOTA
BY

Sofia Karadimitriou

IN PARTIAL FULFILLMENT OF THE REQUIREMENTS
FOR THE DEGREE OF
MASTER OF SCIENCE

Dr. Ioannis Koutlas and Dr. William Oetting, Advisors

August 2015

Acknowledgements

I would like to thank Dr. Ioannis Koutlas for all of his help regarding this project and Dr. William Oetting who never denied any assistance when it was necessary for me.

Dedication

This thesis is dedicated to my mother for her constant support and encouragement.

Abstract

Autosomal dominant mesomandibular fibro-ossseous dysplasia (ADMFOD) is an inherited fibro-osseous condition that affects the mandible and is apparently self-limiting or self-resolving (Koutlas et al., 2012). Two family members, the propositus and his sister, were initially reported by El Deeb et al. as having congenital monostotic fibrous dysplasia (El Deeb et al., 1979). This publication is a follow-up on that family whereby we performed whole exome sequencing on five affected family members in order to identify possible causative gene candidates. We identified seventeen candidate genes and based on either function or association with conditions exhibiting some phenotypic similarities to ADMFOD genes three, *ZSWIM6* (chr.5), *CTBP2* (chr.10), and *CDKN1C* (chr.11) were selected as our best choices. Our results do not support a relation of ADMFOD to fibrous dysplasia since there was no evidence of a *GNAS* mutation. However, we have three other appropriate models under investigation to identify the causative gene and more importantly to elucidate the pathogenesis as well as the mechanism for resolution of these lesions.

Table of Contents

List of Tables

List of Figures

Introduction

Benign fibro-osseous lesions (BFOL) are relatively frequently observed yet most cases are sporadic in the jaws. Such lesions are characterized by replacement of normal bone with cellular fibrous tissue and newly formed osseous (cemento-osseous) deposits. Case reports have been published on families presenting with gigantiform cementomas (Cannon et al., 1980; Young et al., 1989; Oikarinen et al., 1991; Finical et al., 1999), florid osseous dysplasias (Musella and Slater, 1989; Coleman et al., 1996) and periapical cemental dysplasias (Sedano et al., 1982; Thakkar et al., 1993). It is the author's opinion that "familial fibrous dysplasia" as described by Talley et al (Talley 1952) should be reclassified as a form of familial cement-osseous dysplasia, and that the family described by Zohar et al (Zohar et al., 1989) should be considered as just familial cherubism rather than a combination of fibrous dysplasia and cherubism. Fibro-osseous lesions, referred to by some as cemento-ossifying fibromas, have been encountered in patients with hereditary hyperparathyroidism caused by mutations in the tumor suppressor gene *HRPT2* (Rosen and Palmer 1981; Jackson et al., 1990; Aldred et al., 2006).

This publication is a follow-up on that family whereby we performed whole exome sequencing on five affected family members in order to identify possible causative gene candidates. By the same method, absence of a germline *GNAS* mutation and, thus, the distinction of ADMFOD from fibrous dysplasia, can also be reasoned.

Brief description of the pedigree

Figure 1 depicts the family pedigree. A summary of the pedigree is presented here for completeness while more extensive description can be found in the publication by Koutlas et al. (Koutlas et al., 2012).

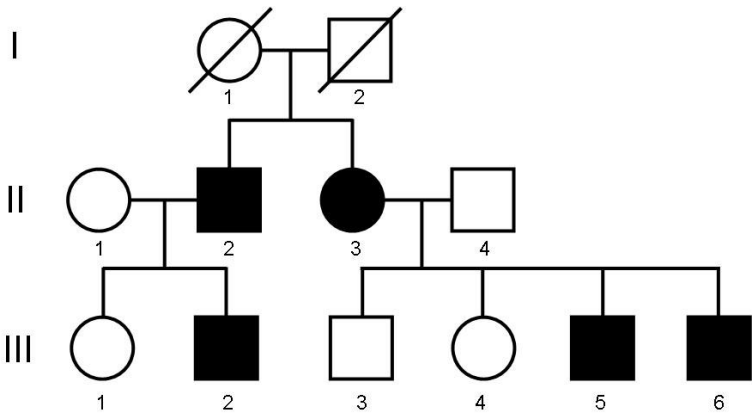

Figure 1. Family pedigree

Male propositus (Patient II-2) was the outcome of a normal pregnancy and delivery in 1976 without any known family history of jaw lesions or consanguinity. He initially presented at three months of age with extensive and progressing congenital enlargement of the anterior middle aspect of the mandible (Figures 2A, B and C) without a significant contributory medical history.

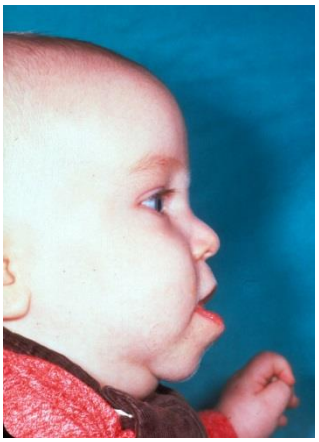

Figure 2A. Male proband at three months of age

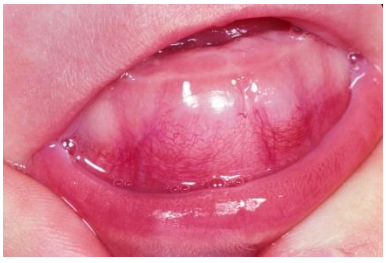

Figure 2B. Enlargement of the anterior middle aspect of the mandible

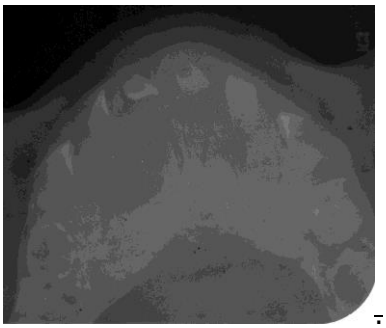

Figure 2C. Radiograph showing mandibular expansion with ill-defined opacification and ground glass appearance.

Serum calcium, phosphorus and alkaline phosphatase levels were found to be within normal limits at the initial evaluation. A biopsy revealed fibroblast-rich collagenous stroma with areas of early osteoid formation and deposits of

irregular spicules of woven bone including limited osteoblastic rimming (Figure 2D). A histological diagnosis was established as a benign fibro-osseous lesion, probable fibrous (fibro-osseous) dysplasia. Follow-up observation was recommended without additional surgical intervention planned at that time.

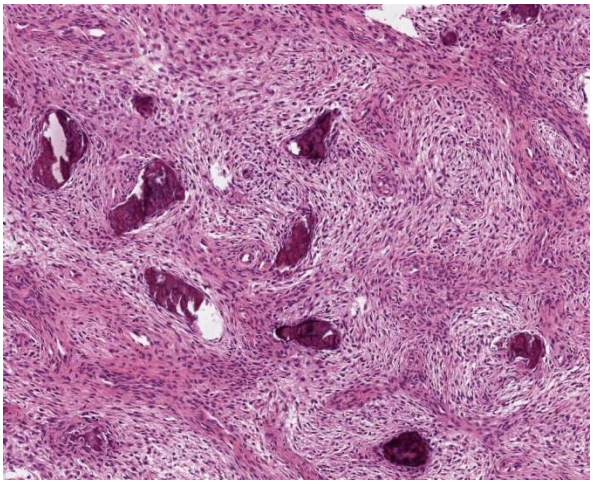

Figure 2D. Collagenous stroma with areas of early osteoid formation and deposits of irregular spicules of woven bone.

At 26 and 36 months (Figure 2E) the lesion showed evidence of regression that was attributed “to the normal growth of the patient”. Throughout this period the patient did not reveal any evidence of café-au-lait spots or other skeletal abnormalities.

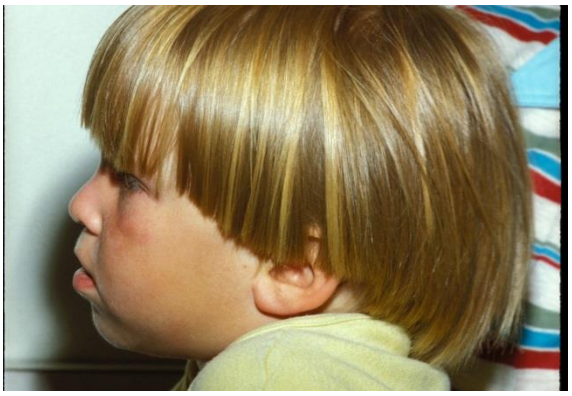

Figure 2E. Profile of male propositus at the age of 36 months.

The male propositus is now 39 years old and does not exhibit any clinical-radiographic lesions of the mandible (Figure 2F). He has two children, an unaffected daughter (III-1) and an affected son (III-2). The son has not undergone any radiographic evaluation or surgical procedures for the lesion, considering the course observed in the father.

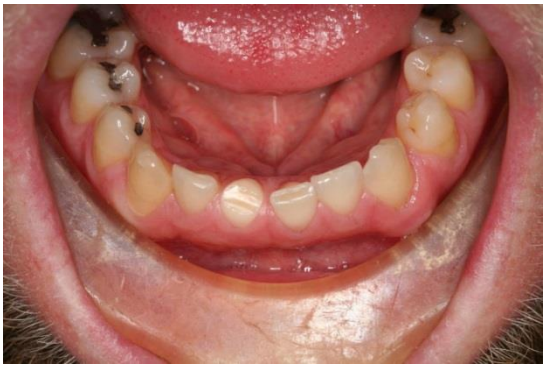

Figure 2F. Male propositus at age 33 years

A two-years younger female sibling of the propositus (Patient II-3) also presented with an essentially similar clinical pathology indicative of congenital mesomandibular enlargement (Figure 3A-C). A biopsy revealed an essentially similar fibro-osseous process.

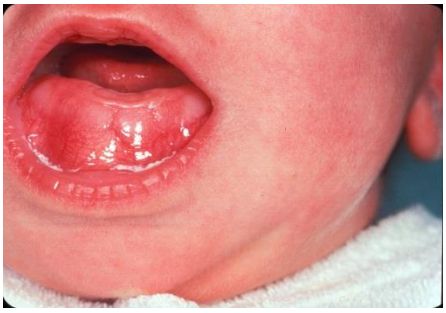

Figure 3A. Female sibling of the propositus at age 12 days.

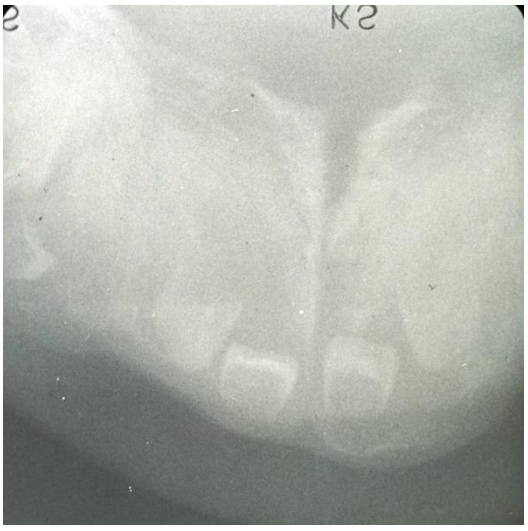

Figure 3B. Ground glass appearance and splaying of teeth.

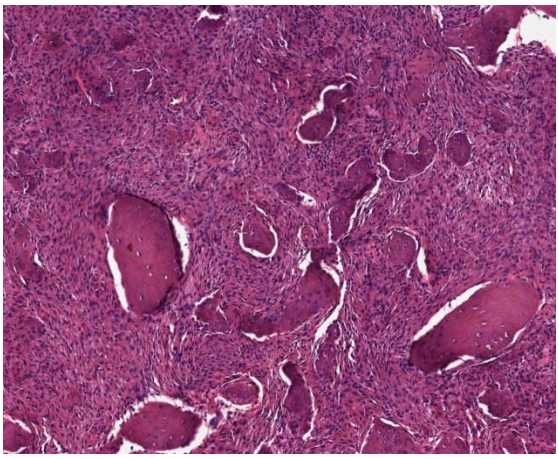

Figure 3C. Fibroblastic proliferation and woven bone spicules with limited osteoblastic rimming.

As of 2013, there isn't any evidence of abnormality for patient II-3 except for transposition of the right mandibular canine and the first premolar.

Two of her male children (Patients III-5 and III-6) presented with the same clinical and histopathologic features. Patient III-5 was also noticed to exhibit left sided limb enlargement (1 cm leg size discrepancy) at 12 months as well as slight asymmetry between the right and left hands and right and left feet. Radiographic evaluations of the chest, pelvis, hands and feet including bone length studies were undertaken from 2007 to 2011. The final bone length analysis revealed a 0.9 cm discrepancy between the left and the right extremities. Specifically, the measurement from the right superior femoral head to the tibial plafond was 54.4 cm while the left measured 55.3 cm. The left femur and tibia were each 0.5 cm longer than the right, respectively. The patient also presented with bilateral coxa

valga deformities that have shown improvement with time. A chest evaluation did not reveal any abnormalities or osseous structures. It is unclear if these skeletal abnormalities are part of the condition since none of the other affected members of the pedigree exhibited these skeletal deformities.

METHODS AND MATERIALS

The study design for this investigation was submitted to the University of Minnesota's IRB and grant approval (IRB#:1206M15601). DNA was extracted from peripheral white blood cells from patients II-2, II-3, III-2, III-5 and III-6 while DNA was also extracted from the spouses of patients II-2 and II-3. Study of phenotypical normal children III-1, III-3 and III-4 were excluded by IRB restrictions.

Sample Quality Assessment and Library Preparation

Genomic DNA samples were quantified using a fluorimetric PicoGreen assay. To pass quality control samples had to contain >3 µgrs of DNA and display an A260:280 ratio above 1.7. Control samples had to contain >3 µgrs of DNA and display an A260:280 ratio above 1.7 to pass quality. Libraries for Illumina Next-Generation Sequencing were generated using the SureSelect XT Reagent Kit, HSQ (G9611A) (Agilent Technologies, Santa Clara, CA) following SureSelectXT Target Enrichment System for Illumina Paired End Sequencing Library User's Guide Version 1.4.1 from Agilent Technologies (Agilent Techologies). Three

µgrs of genomic DNA were sheared using the Covaris system to an average size of 200 base pairs and sheared samples were end-repaired, a-tailed, and ligated to adapters (Agilent Technologies). Adaptor-ligated libraries were amplified by PCR using Herculase Fusion DNA Polymerase (Agilent Technologies). The amplified libraries were then analyzed for quality and quantity using a Bioanalyzer and fluorimetric PicoGreen assay. In order to pass quality control, libraries had to contain more than 750 nanograms and have an average peak size between 250 - 275 bp.

Hybridization and Sequence Capture

A quantity of 750 nanograms of amplified material was hybridized to biotinylated oligonucleotide probes complementary to regions of interest (SureSelectXT Human All Exon V5+UTRs, 5190-6213) at 65 degrees Celsius for 24 hours. Subsequently, library-probe hybrids were pulled down using streptavidin-coated magnetic beads and subjected to multiple washing steps to remove non-specifically bound material. The captured material was amplified by PCR using Herculase Fusion DNA Polymerase (Agilent Technologies). Captured, amplified libraries underwent quality control using a Bioanalyzer, and fluorimetric PicoGreen assay. Libraries were considered to pass this quality control as long as they contained more than 10 nM of library and had an average peak size between 300- 400 bp.

Cluster generation and sequencing

Libraries were hybridized to a paired end flow cell at a concentration of 10 pM. Individual fragments were clonally amplified by bridge amplification on the Illumina cBot. Amplified fragments were sequenced on the HiSeq 2000 or 2500 using Illumina's SBS chemistry (Illumina, San Diego, CA). Upon completion of read 1, a 7 base pair index read was performed. The library fragments were then resynthesized in the reverse direction and sequenced from the opposite end of the read 1 fragment, thus producing the template for paired end read 2.

Primary analysis and de-multiplexing

Base call (.bcl) files for each cycle of sequencing were generated by Illumina Real Time Analysis (RTA) software and run folders were then exported to servers maintained at the Minnesota Supercomputing Institute. Primary analysis and de-multiplexing were performed using Illumina's CASAVA software 1.8.2.

Sequence Quality Control

All multiplexed samples were individually evaluated for sequence quality using FastQC. The majority of sequence files were of excellent quality. A small subset of files showing extremely poor quality corresponded to the first pass of a subset of samples that were resequenced due to a failed sequencing run. These resequenced versions were much improved. All samples were trimmed for low quality ends (PHRED score < 20) via an in house script. Contaminating adapter

fragments of all samples were trimmed via the Cutadapt software package using default parameters and the TruSeq (Illumina) adapter sequences.

Mapping The BWA sequence mapper was used to map sequences to the human reference genome. The resulting BAM files were annotated with LANEID information and SAMPLEID information as required for the read groups in subsequent analysis steps.

Read Recalibration

The BAM alignment files were: a) stripped of duplicate reads, unmapped reads, and low average quality reads, b) realigned for sequence regions marked as potential indels via the GATK IndelRealigner and, c) recalibrated for per base calls to address systemic biases utilizing the Broad Institute's (Massachusetts Institute of Technology, Harvard University Collaborative) published best practices for the Genome Analysis Toolkit (GATK) variant calling pipeline. This was performed on a per sequencing lane basis with grouping of multiple samples. Recalibration was driven by looking at true positives as identified in dbSNP. Detected systemic biases were subsequently corrected.

Haplotype Calling and Variant Detection Utilizing error information from all samples, all variants were called together. Regions with less than an average of 10x coverage per patient were excluded and samples with coverage over 250x were subsampled to 250x coverage.

Variant Recalibration

Single nucleotide polymorphisms call scores were recalibrated and filtered based on information in hapmap, OMIM and dbSNP. A similar recalibration was applied independently to called indels.

Variant Annotation

All variants detected were annotated using the AnnoVar package. Annotation data sources included: a) 1000genomes, b) refGene, c) PHAST, d), SIFT e) genomicSuperDups (Segmental Duplications), f) ExomeVariantServer, and g) Polyphen.

Variant Filtering

Variants were filtered based on the assumption of autosomal dominant inheritance of the genotype within the families (as opposed to de novo). Based on this assumption, only those variants showing the proper segregation with the phenotype in the family were considered as possible causal variants.

RESULTS

Seventeen candidate genes containing mutations were identified based on their segregation with the phenotype and potential for being functional. These mutations were common in both the propositus II-2, his sister II-3 and their affected children. They are summarized in TABLE 1. They were not present in the spouses. Searching through the Gene Cards database (http://www.genecards.org) confirmed that all genes identified are protein coding. Among them, we selected *ZSWIM6* (chr.5; exon1:c.82_83insGCG:p.S28delinsSG), *CTBP2* (chr.10; exon5:c.G2272T:p.E758X;) and *CDKN1C* (chr.11; exon1:c.512_523del:p.171_175del;) as possible causative gene candidates for ADMFOD.

Table 1.

Chr	Gene	Exonic Function	Amino Acid Change	Function/Role/Associated Diseases
chr1	NBPF1	unknown	UNKNOWN	Associated with developmental and neurogenetic diseases: microcephaly, macrocephaly, autism, schizophrenia, mental retardation, congenital heart disease, neuroblastoma, and congenital kidney and urinary tract anomalies. Altered expression of some gene family members is associated with several types of cancer.
chr2	SLC4A10	nonsynonymous SNV	exon21:c.T2945C:p.M982T,SLC4A10:NM_001178015:exon22:c.T3035C:p.M1012T,SLC4A10:NM_001178016:exon22:c.T2978C:p.M993T	Regulates the intracellular pH of neurons, the secretion of bicarbonate ions across the choroid plexus and the pH of the brain extracellular fluid. Among its related pathways are transport of glucose and other sugars, bile salts and organic acids, metal ions and amine compounds. Associated diseases include complex partial epilepsy. Associated diseases include polydactyly, postaxial, type a6 and postaxial polydactyly type a, bilateral.
chr4	ZNF141	nonsynonymous SNV	exon3:c.T163A:p.C55S	May be involved in transcriptional regulation as a repressor. Plays a role in limb development.
chr4	ZNF141	nonsynonymous SNV	exon3:c.G193T:p.V65L	Same as above
chr4	ZNF141	frameshift insertion	exon3:c.204_205insGA:p.H68fs	Same as above
chr4	ZNF141	nonsynonymous SNV	exon3:c.G207C:p.K69N	Same as above
chr4	ZNF141	frameshift deletion	exon3:c.209_210del:p.70_70del	Same as above
chr4	ZNF141	nonsynonymous SNV	exon3:c.T212C:p.V71A	Same as above
chr5	BRD9	nonsynonymous SNV	exon8:c.C713T:p.T238M,BRD9:NM_023924:exon8:c.C872T:p.T291M	Associated diseases include shipyard eye and rhabdomyosarcoma. May play a role in chromatin remodeling and regulation of transcription.
chr5	ZSWIM6	nonframeshift insertion	exon1:c.82_83insGCG:p.S28delinsSG	Associated diseases include acromelic frontonasal dysostosis.
chr9	ANKRD18B	nonsynonymous SNV	exon13:c.A2425G:p.K809E	
chr9	FAM205A	nonsynonymous SNV	exon4:c.A2168T:p.E723V	
chr10	CTBP2	stopgain SNV	exon5:c.G2272T:p.E758X,CTBP2:NM_001083914:exon7:c.G652T:p.E218X,CTBP2:NM_001329:exon7:c.G652T:p.E218X	Corepressor targeting diverse transcription regulators. Functions in brown adipose tissue differentiation.
chr11	KRTAP5-5	frameshift deletion	exon1:c.525_528del:p.175_176del	In the hair cortex, hair keratin intermediate filaments are embedded in an interfilamentous matrix, consisting of hair keratin-associated protein (KRTAP), which are essential for the formation of a rigid and resistant hair shaft through their extensive disulfide bond cross-linking with abundant cysteine residues of hair keratins. The matrix proteins include the high-sulfur and high-glycine-tyrosine keratins. No associated diseases found.
chr11	KRTAP5-5	frameshift deletion	exon1:c.530_555del:p.177_185del	Same as above

chr11	CDKN1C	nonframeshift deletion	exon1:c.512_523del:p.171_175del,CDKN1C:NM_001122630:exon2:c.479_490del:p.160_164del,CDKN1C:NM_001122631:exon2:c.479_490del:p.160_164del	This gene is imprinted, with preferential expression of the maternal allele. The encoded protein is a tight-binding, strong inhibitor of several G1 cyclin/Cdk complexes and a negative regulator of cell proliferation. Among its related pathways are Endochondral Ossification and Cell Cycle / Checkpoint Control and to lesser extent, of the mitotic cyclin B-CDC2. May play a role in maintenance of the non-proliferative state throughout life. Associated diseases are Image syndrome and Beckwith-Wiedemann syndorome, suggesting that this gene is a tumor suppressor candidate. It is also implicated in sporadic cancers.
chr11	PDE3B	nonsynonymous SNV	exon16:c.G3167A:p.R1056Q	Involved in signaling by GPCR (G-protein-coupled receptor) and Insulin receptor signalling cascade and many signal transduction pathways. Functions include vascular smooth muscle proliferation and contraction, cardiac contractility, platelet aggregation, hormone secretion, immune cell activation and involvement in learning and memory. May play a role in fat metabolism.

Although ZNF141 is associated with limb development it was excluded because it was found to be a paralog in another gene-related project that our group has been working on, focal palmoplantar and masticatory (gingival) hyperkeratosis. We also excluded the thirteen other genes because they are related to conditions that feature phenotypes which do not share common clinical manifestations with the patients in our study. We did not consider genes unassociated with the BMP pathway as likely candidates. Importantly, WES did not provide any evidence of *GNAS* mutation for ADMFOD and thus any relation to fibrous dysplasia could not be established.

DISCUSSION

A review of the records for the two propisiti with ADMFOD indicated that they were initially diagnosed as an autosomal recessive form of congenital fibrous dysplasia (ElDeeb, 1979) due to lack of a better diagnosis. Indeedpathology reports at that time included extensive commentary on the unusual histopathologic features of the lesions which did not fully support the diagnosis of fibrous dysplasia.

It is well known now that syndromes featuring fibrous dysplasia (McCune-Albright, Jaffe syndrome) as well as monostotic cases are caused by somatic (postzygotic) mutations of the gene encoding the alpha subunit of the stimulatory G protein, $G_s\alpha$, on chromosome 20 (Weinstein et al., 1991; Riminucci et al.,

2007). These mutations replace arginine in codon 201 with either cysteine or histidine in most cases. It has also been shown that individual lesions of fibrous dysplasia are themselves a mosaic of mutated and normal cells (Bianco et al., 1998). With time, the population of mutated cells decreases while normal cells predominate thus leading to arrested growth of lesions. The bone morphogenetic protein (BMP) signaling pathway is also involved in the pathogenesis of these lesions (Kiss et al., 2010) with differences in the expression of BMP2, BMP4, BMPR1A, BMPR2, and other members of the pathway observed between subjects with and without fibrous dysplasia associated disorders. It has also been postulated that since mutant cells in fibrous dysplasia are clonal fibroblast-like osteoprogenitor cells demonstrating high expression of the c-fos proto-oncogene, fibrous dysplasia should be considered a neoplasm (Cohen, 2001).

There are rare familial cases of fibrous dysplasia which include two monozygotic twins, one with McCune-Albright, the other with limited fibrous dysplasia (Lemli 1977), a family with only craniofacial involvement (Reitzik and Lownie, 1975), two siblings with polyostotic disease (Sarkar et al., 1993) and the pedigree described by Alvarez-Arratia et al (Alvarez-Arratia et al., 1983), in which only one of the patients appeared to have convincing disease. If these are true cases of familial fibrous dysplasia they are either the result of gametic half chromatid mutation or hereditary conditions caused by a presently unknown gene mutation that presents a phenotype similar to fibrous dysplasia. The only pedigree

investigated for *GNAS* mutation without succeeding identifying any (Mangion et al., 2000), is the family presented by Pierce et al (Pierce et al., 1985). They concluded that “craniofacial fibrous dysplasia is a different entity from other forms of fibrous dysplasia” (Mangion et al., 2000), a misleading statement in our opinion, since there are several sporadic cases of craniofacial fibrous dysplasia associated with *GNAS1* mutations identified in lesional tissue (Toyosawa et al., 2007; Idowu et al., 2007). Based on the published clinical, radiographic and histologic figures it appears that the family described by Pierce et al (Pierce et al., 1985) and followed for many years (Pierce et al., 1996), represents either familial florid osseous dysplasia or a unique entity certainly different from fibrous dysplasia. If feasible, linkage studies in the aforementioned families are necessary to confirm the proposed diagnoses of familial fibrous dysplasia.

We argue against the diagnosis of familial monostotic fibrous dysplasia because as we can see in our pedigree under investigation the a) unlikelihood of true familial cases of monostotic fibrous dysplasia, b) occurrence of the lesion in the mandibular midline, hardly a preferred site for fibrous dysplasia, and c) clinical behavior, featuring a self-limiting or self-resolving process. The name autosomal dominant mesomandibular fibro-osseous dysplasia is the term we prefer to best describe the condition. We have elected not to refer to the process as osteofibrous dysplasia, to distinguish it from the familial form of osteofibrous dysplasia (Karol et al., 2005; Hunter and Jarvis, 2002) a benign bone dysplastic

process affecting primarily the cortex of the tibia and/or the fibula of skeletally immature patients, i.e. children and neonates and characterized by anterolateral bowing of the affected bones that often leads to fractures and development of pseudoarthroses especially if the fractures occur before the first birthday of patients (Karol et al., 2005). Osteofibrous dysplasia is histologically characterized by fibroblastic proliferation associated with woven bone rimmed by osteoblasts, the latter not being a consistent feature of fibrous dysplasia. Nor have cases of osteofibrous dysplasia shown any *GNAS* mutation (Sakamoto et al., 2000).

Previously, we postulated that a gene involved in the BMP pathway and specifically in the formation of the middle region of the mandible may be that culprit (Koutlas et al. 2012). WES identified seventeen genes, summarized in Table 1, that are altered in all affected members of our pedigree. Among them three loci, *CTBP2, ZSWIM6*, and *CDKN1C*, were considered possible candidates since they may be related to the BMP pathway.

C-terminal binding proteins (CtBPs) are a group of proteins that bind to the C-terminal region of the human adenovirus E1A proteins via the highly conserved PLDLS motif. CtBPs, when acting in the nucleus, are transcriptional corepressors that interact with many DNA binding transcription factors, including mediators of Wnt, BMP, and Notch signaling, GATA transcription factors,

regulators of several key processes, include control of segmentation, somitogenesis, neural tube and limb patterning, vascularization, apoptosis, cell adhesion, and gene activation (Van Hateren et al, 2006). In the cytoplasm, CtBPs are primarily regulators of the Golgi apparatus fission (Bergman et al., 2009).

Two members of the CtBP family have been identified in humans, CTBP1 (the original E1A-interacting CtBP) and CtBP2. Early in embryologic development, CtBP1 and CtBP2 are expressed in the primitive streak and neural plate as well as the dorsal neural tube and roof plate and contribute to morphologic pattern regulation. Mouse embryos lacking CtBP1 are small but viable, whereas CtBP2-deficient embryos die at midgestation and display defective development of several tissues, including truncations of axial mesoderm. CtBP2 expression is detected in the head process and although both CtBP1 and CtBP2 are expressed in the ectoderm and mesoderm, CtBP2 expression is more abundant in the mesodermal layer. CtBP2 expression displays also a dynamic pattern as somites mature as well as in avian forelimb and hindlimb development. CtBP1 interacts with Smad6 and this can have an effect in BMP. Specifically, the BMP-2 pathway can be repressed by Smad- CtBP1 interaction. The association of CtBP1 with Smad6 occurs through binding of the PLDLS motif in the linker region of Smad6. Mutations in the PLDLS motif abolish the ability of Smad6 to bind CtBP and consequently decrease Smad6 capacity for inhibiting BMP signaling

(Lin et al., 2003). Although the interaction of CtBP2 and Smad6 is currently unknown it appears plausible that such interplay may also affect BMP and, thus, mutations in CtBP2 will consequently affect BMPs. Such mutations in CtBP2 can contribute to the formation of the mesomandibular fibro-osseous lesions, as well as the skeletal asymmetry seen in one of the patients (patient III-5).

ZSWIM6 encodes a 133.5 kDa protein containing a zinc finger SWIM domain which has DNA binding and protein-protein interaction functions (Makarova KS, Aravind L, Koonin EV, 2002). Proteins with such domains have been identified in a variety of organisms, from bacteria to eukaryotes. However, little is known about the function of SWIM proteins. Recently, by performing WES, Smith et al. (Smith et al., 2014) identified a c.3487C>T (p. Arg1163Trp) in a highly conserved protein domain of *ZSWIM6* in members of a family with acromelic frontonasal dysostosis, a type of frontonasal dysplasia, presenting also with interhemispheric lipoma, agenesis of the corpus callosum, tibial hemimelia, preaxial polydactyly of the lower limbs and various levels of intellectual disability. RNA in situ hybridization on zebrafish found telencephalic midbrain, hindbrain, and retinal expression of *ZSWIM6* very early in embryogenesis while immunohistochemistry in mice disclosed positive staining in the lens fiber cells and in the stereocilia of the outer hair cells of the cochlea, a subpopulation of cells in the external root sheath of the hair follicle, ameloblasts and odontoblasts and a subset of skeletal-muscle cells. By performing qRT-PCR expression analysis of osteoblast and

fibroblast cell lines available from two probands, Smith et al. suggested activation of the Hedgehog signaling pathway and the identified c.3487C >T SNV was regarded as a gain of function mutation. Disturbance of the Hedgehog pathway in patients with acromelic dysostosis was also proposed by Slaney et al, 1999 and Hing et al, 2004.

In our kindred the mutation was characterized by a three nucleotide insertion, GCG, in between the DNA bases 82 and 83. According to Kunkel, 1985 and Oetting et al, 1991, frameshift mutations can easily occur at repetitive base sequences and at a very high frequency. According to Kunkel's model, the repetitive sequence allows for slippage and misalignment of the strands of the DNA, with a looping out of one or more bases. Subsequent DNA synthesis would either omit or add a nucleotide or a nucleotide pair (TABLE 2).

	Nucleotide Bases
Normal DNA	ATGGCGGAGC GCGGACAGCA GCCTCCTCCC GCGAAACGGC TTTGCTGCCG GCCGGGCGGC GGCGGCGGCG GCGGGGGCAG CAGCGGCGGC GGCGGCGGCG CGGGTGGCGG CTACAGCTCT GCCTGTCGGC CAGGCCCGCG GGCGGGTGGC GCGGCGGCGG CGGCGGCGTG CGGGGGCGGC
Mutated DNA	ATGGCGGAGC GCGGACAGCA GCCTCCTCCC GCGAAACGGC TTTGCTGCCG GCCGGGCGGC GGCGGCGGCG GCGGGGGCAG CAGCGGCGGCGGC GGCGGCGGCG CGGGTGGCGG CTACAGCTCT GCCTGTCGGC CAGGCCCGCG GGCGGGTGGC GCGGCGGCGG CGGCGGCGTG CGGGGGCGGC

TABLE 2. Insertion of GCG and comparison between normal and mutated DNA

In our case, the GCG bases on the DNA sequence are the codon that translates into alanine (Ala/A) on the relevant proteinic product. The common DNA sequence (http://www.ncbi.nlm.nih.gov/protein/NP_065979.1) that is found in the general population is translated into:

```
1   maergqqppp akrlccrpgg ggggggssgg gggagggyss acrpgpragg aaaaaacggg
61  aalgllppgk tqspeslldi aarrvaekwp fqrveerfer ipepvqrriv ywsfprsere
121 icmyssfntg ggaaggpgdd sgggggaggg ggggsssspa atsaaatsaa aaaaaaaaaa
181 aaaagagaps vgaagaadgg detrlpfrrg iallesgcvd nvlqvgfhls gtvtepaiqs
241 epetvcnvai sfdrckitsv tcscgnkdif ycahvvalsl yrirkpdqvk lhlpisetlf
301 qmnrdqlqkf vqylitvhht evlptaqkla deilsqnsei nqvhgapdpt agasiddenc
361 whldeeqvqe qvklflsqgg yhgsgkqlnl lfakvremlk mrdsngarml tliteqfmad
421 prlslwrqqg tamtdkyrql wdelgalwmc ivlnphckle qkaswlkqlk kwnsvdvcpw
481 edgnhgselp nltnalpqga nanqdssnrp hrtvftraie acdlhwqdsh lqhiissdly
541 tnycyhddte nslfdsrgwp lwhehvptac arvdalrshg yprealrlai aivntlrrqq
601 qkqlemfrtq kkelphknit sitnlegwvg hpldpvgtlf sslmeacrid denlsgfsdf
```

In our case, the addition of the alanine would take place in the depicted area of the twenty-seventh amino acid (TABLE 3)

	Amino Acids
Normal Protein	maergqqppp akrlccrpgg ggggggssgg gggagggyss acrpgpragg aaaaaacggg aalgllppgk tqspeslldi aarrvaekwp fqrveerfer ipepvqrriv ywsfprsere
Altered Protein	maergqqppp akrlccrpgg ggggggs**a**sgg gggagggyss acrpgpragg aaaaaacggg aalgllppgk tqspeslldi aarrvaekwp fqrveerfer ipepvqrriv ywsfprsere

TABLE 3: Addition of alanine alters the amino acid sequence

Such an addition could be altering the structure of the *ZSWIM6* protein and hence, its functionality. Specifically, alanine (Ala or A) is an α-amino acid with (CH3CH(NH2)COOH) and is classified as a non-polar amino acid. Its methyl group (-CH3), classifies alanine as an aliphatic amino acid. The methyl group of alanine is non-reactive and thus it is almost never directly involved in protein function. On the other hand, serine (Ser or S, HO2CCH(NH2)CH2OH) is a proteinogenic amino acid. By virtue of the hydroxyl group, serine is classified

as a polar amino acid. The amino-acid insertion happened in an area of repeated glycine residues. Glycine (Gly or G, NH2CH2COOH), having a hydrogen substituent as its side-chain, is the smallest of the twenty amino acids commonly found in proteins. It can fit into hydrophilic or hydrophobic environments, due to its minimal side chain of only one hydrogen atom. This difference in the biochemical structure of A and S amino-acids might be implicated in the altered protein structure here. Specifically, the insertion of an aliphatic amino-acid in-between two polar amino-acids could possibly force the polypeptidic chain (primary structure) to "fold" in a different area than normal, changing its secondary and tertiary structure. Unfortunately, at this point we cannot predict the biological consequences of such alteration. It might be for example, that this ZSWIM6 role is to repress an enzymatic reaction and now, due to its altered structure, cannot be functional anymore, leading to the increased or excessive production of an abnormal biological product. Alternatively, ZSWIM6 might be involved in a cascade of biochemical reactions that could be eventually suppressing the expression of a gene and now with the protein's altered form and decreased or depleted functionality, the gene expression is inadvertently upregulated, resulting in, for example, abnormal proliferation of fibroblasts or osteoblasts and abnormal ossification as seen in our patients.

Smith et al (Smith et al., 2014) sequence analysis of ZSWIM6 predicts an all-α-helical structure with novel fold topology. One poly-alanine and two poly-glycine

repeats occur in the N-terminal 200 residues of the protein, for which a disordered or extended structure was predicted. The authors by using the CADD score, which can predict the impact of the mutation on protein function, and through an in silico analysis, showed that the substitution of arginine by tryptophan dramatically altered the structure and hydrophobicity of the protein encoded by *ZSWIM6*. So, in that case, the mutation was a non-frameshift substitution. In our case though, we have a non-frameshift insertion of three bases, which adds a whole new amino-acid in the final protein.

It is important to examine whether the area of the observed mutation is a conserved area among different species or not. In order to see whether this area is conserved and to check which animal species we could further experiment with in order to examine the possibility that we could re-create the same phenotype as the members of the family which we have here, we examined the homology of the ZSWIM6 gene and performed a protein alignment within several species on the ncbi.gov website (specifically, http://www.ncbi.nlm.nih.gov/homologene?cmd=Retrieve&dopt=MultipleAlignment&list_uids=83517). Table 4 shows the alignment of amino acids in the region of interest where the three base insertion takes place. It appears that this area is conserved only in the mouse.

Species	Amino Acid Sequence
Human	MAERGQQPPPAKRLCCRPGGGGGGGSSGG--GGGAGGGYSSACRPGPRA
Wolf	----------MTAKL
Bull	----------M
Mouse	MAERGQQPPPAKRLCCRPGGGGGGGGGGGSSGGGAGGGYSSACRPGPRA
Rat	----------
Chicken	MAERGQLPPPAKRLCCRP----------GYGSGCRPGGRV
Zebrafish	MAER-VLQPAAKRLCCRP----------GYGSTCRPGQRL
Frog	MSRYPWLDLNTH----------AGFRTEFVWSCPRGPAF

TABLE 4: Alignments of amino acids in diverse species

CDKN1C (Cyclin-Dependent Kinase Inhibitor 1C) encodes a cyclin-dependent kinase inhibitor p57 (KIP2) that negatively regulates cellular proliferation. It is regarded as a tumor suppressor gene and is paternally imprinted with preferential expression of the maternal allele. Mutations of the gene have been seen in cases of IMAGE syndrome characterized by intrauterine growth retardation, failure of adolescent growth spurt with proportional adult short stature, minimal subluxation of the fifth metacarpal-phalangeal joint, and adult-onset diabetes unrelated to obesity or other signs of metabolic syndrome, as well as, in Beckwith-Wiedemann which in contrast is an overgrowth syndrome with patients featuring disproportionate limb growth, occasional hemihypertrophy, macroglossia, omphalocele, neonatal hypoglycemia and pediatric tumors that include Wilm's tumor, hepatoblastoma and pancreatoblastoma. Also, in mice lacking imprinted *CDKN1C* besides visceromuscular defects there is evidence of impaired endochondral ossification, cleft palate and incomplete differentiation of chrondrocytes (Zhang et al., 1997). Although mandibular ossification is

intramembranous, there is still possibility that a CDKN1C defect may induce the overgrowth observed in our patients.

Conclusions

In summary, three genes *ZSWIM6, CDKN1C and CTBP2,* were identified by WES as potential candidates for ADMFOD. A unique feature in the patients with ADMFOD is that the lesions reverse or that bony tumors disappear because of termination of mutated gene activity and repair by normal bone growth. This feature by itself separates ADMFOD from other benign osseous dysplasias such as fibrous dysplasia and segmental odontomaxillary dysplasia where there is arrest of abnormal bone growth after a certain age. WES did not provide evidence of $G_s\alpha$ mutation and thus any genetic commonality between ADMFOD and FD could not be established. Further studies are underway to confirm one of three genes discussed above as the cause for ADMFOD and more importantly the spatiotemporal mechanism leading to the growth and arrest of the lesions.

REFERENCES

Al-Adnani M, Idowu B, Yu L, Diss TC, Gale RE, Odell E, Flanagan AM. 2005. A simple and reliable method for the molecular diagnosis of fibrous dysplasia. Mod Pathol 18(S):10A-11A.

Aldred MJ, Talacko AA, Savarirayan R, Murdolo V, Mills AE, Radden BG, Alimov A, Villablanca A, Larsson C. 2006. Dental findings in a family with hyperparathyroidism-jaw tumor syndrome and a novel HRPT2 gene mutation. Oral Surg Oral Med Oral Pathol 101:212-218.

Alvarez-Arratia MC, Rivas F, Avila-Abundis RA, Hernández A, Nazará Z, López C, Castillo A, Cantú JM. 1983. A probable monogenic form of polyostotic fibrous dysplasia. Clin Genet 24:132-139.

Balemans, W. and Van Hul, W. 2002. Extracellular regulation of BMP signaling in vertebrates: a cocktail of modulators. Dev Biol 250:231-250.

Bergman LM, Birts CN, Darley M, Gabrielli B, Blaydes JP. 2009. CtBPs promote cell survival through the maintenance of mitotic fidelity. Mol Cell Biol. 2009 Aug;29(16):4539-51.

Bianco P, Kuznetsov S, Riminucci M, Fisher LW, Spiegel AM, Geron Robey P. 1998. Reproduction of human fibrous dysplasia of bone in immunocompromised mice by transplanted mosaics of normal and Gs-alpha mutated skeletal progenitor cells. J Clin Invest 101:1737-1744.

Campanacci M, Laus M. 1981. Osteofibrous dysplasia of the tibia and fibula. J Bone Joint Surg Am 63:367-375.

Cannon JS, Keller EE, Dahlin DC. 1980. Gigantiform cementoma: report of two cases (mother and son). J Oral Maxillofac Surg 38:65-70.

Chatterjee SK, Mazumder JK. 1967. Massive fibro-osseous dysplasia of the jaws in two generations. Br J Surg 54:335-340.

Cohen MM Jr. 2001. Fibrous dysplasia is a neoplasm. Am J Med Genet 98:290-293.

Coleman H, Altini M, Kieser J, Nissenbaum M. 1996. Familial florid cemento-osseous dysplasia--a case report and review of the literature. J Dent Assoc S Afr 51:766-770.

Finical SJ, Kane WJ, Clay RP, Bite U. 1999. Familial gigantiform cementoma. Plast Reconstr Surg 103:949-954.

El Deeb M, Waite DE, Gorlin RJ. 1979. Congenital monostotic fibrous dysplasia-a new possibly autosomal recessive disorder. J Oral Maxillofac Surg 37:520-525.

Ferguson CA, Tucker AS, Sharpe PT. 2000. Temporospatial cell interactions regulating mandibular and maxillary arch patterning. Development 127:403-412.

Fukuda T, Kohda M, Kanomata K, Nojima J, Nakamura A, Kamizono J, Noguchi Y, Iwakiri K, Kondo T, Kurose J, Endo K, Awakura T, Fukushi J, Nakashima Y, Chiyonobu T, Kawara A, Nishida Y, Wada I, Akita M, Komori T, Nakayama K, Nanba A, Maruki Y, Yoda T, Tomoda H, Yu PB, Shore EM, Kaplan FS, Miyazono K, Matsuoka M, Ikebuchi K, Ohtake A, Oda H, Jimi E, Owan I, Okazaki Y, Katagiri T. 2009. Constitutively activated ALK2 and increased SMAD1/5 cooperatively induce bone morphogenetic protein signaling in fibrodysplasia ossificans progressiva. J Biol Chem 284:7149-7156.

Gartler SM, Francke U. Half chromatid mutations: transmission in humans? Am J Hum Genet 1975;27:218-223.

Happle R. 1987. Lethal genes surviving by mosaicism: A possible explanation for sporadic birth defects involving the skin. J Am Acad Dermatol 16:899-906.

Hing AV, Syed N, Cunningham ML. 2004. Familial acromelic frontonasal dysostosis: autosomal dominant inheritance with reduced penetrance. Am J Med Genet A. 2004 Aug 1;128A(4):374-82.

Hsissen MA, Kadiri F, Zamiati S, Jabri L, Rifki S, Touhami M, Chekkoury IA, Benchakroun Y. 1997. A propos d'un cas de dysplasia fibreuse faciale dans une fatrie. Rev Stomatol Chir Maxillofac 98:96-99.

Hunter AG, Jarvis J. 2002. Osteofibrous dysplasia: two affected male sibs and an unrelated girl with bilateral involvement. Am J Med Genet 112:79-85.

Idowu BD, Al-Adnani M, O'Donnell P, Yu L, Odell E, Diss T, Gale RE, Flanagan AM. 2007. A sensitive mutation-specific screening technique for *GNAS1* mutations in cases of fibrous dysplasia: the first report of a codon 227 mutation in bone. Histopathology 50:691-704.

Jackson CE, Norum RA, Boyd SB, Talpos GB, Wilson SD, Taggert RT, Mallette LE. 1990. Hereditary hyperparathyroidism and multiple ossifying jaw fibromas: a clinically and genetically distinct syndrome. Surgery 108:1006-1013.

Karol LA, Brown DS, Wise CA, Waldron M. 2005. Familial osteofibrous dysplasia. A case series. J Bone Joint Surg Am 87:2297-2307.

Kiss, J., Balla, B., Kosa, J. P., Borsy, A., Podani, J., Takacs, I., Lazary, A., Nagy, Z., Bacsi, K., Kis, A. et al. 2010. Gene expression patterns in the bone tissue of women with fibrous dysplasia. Am J Med Genet A 152A:2211-2220.

Koutlas IG, Forsman CL, Kyrkanides S, Oetting WS, Petryk A. 2012. Autosomal dominant mesomandibular fibro-osseous dysplasia: a self-resolving inherited fibro-osseous lesion of the jaws. Front Physiol 6:458

Kundu JP, Pan AK. 1979. Congenital fibro-osseous dysplasia of jaws ("hippopotamus face"). An anaesthetic problem. Br J Anaesth 51:465-467.

Kunkel TA. 1985. The mutational specificity of DNA polymerase-beta during in vitro DNA synthesis. Production of frameshift, base substitution, and deletion mutations. J Biol Chem. 1985 May 10;260(9):5787-96.

Lemli L. 1977. Fibrous dysplasia of bone. Report of female monozygotic twins with and without the McCune-Albright syndrome. J Pediatr 91:947-949.

Lenz W. Letter: Half chromatic mutations may explain incontinentia pigmenti in males. Am J Hum Genet 1975;27:690-691.

Lin X, Liang YY, Sun B, Liang M, Shi Y, Brunicardi FC, Shi Y, Feng XH. 2003. Smad6 recruits transcription corepressor CtBP to repress bone morphogenetic protein-induced transcription. Mol Cell Biol 23:9081-93.

MacKenzie B, Wolff R, Lowe N, Billington CJ, Jr., Peterson A, Schmidt B, Graf D, Mina M, Gopalakrishnan R, Petryk A. 2009. Twisted gastrulation limits apoptosis in the distal region of the mandibular arch in mice. Dev Biol 328:13-23.

Makarova KS, Aravind L, Koonin EV. 2002. SWIM, a novel Zn-chelating domain present in bacteria, archaea and eukaryotes. Trends Biochem Sci. 2002 Aug; 27(8):384-6.

Mangion J, Edkins S, Goss AN, Stratton MR, Flanagan AM. 2006. Familial craniofacial fibrous dysplasia: absence of linkage to *GNSA1* and the gene for cherubism. J Med Genet 37:e37

Mina M, Wang YH, Ivanisevic AM, Upholt WB, Rodgers B. 2002. Region- and stage-specific effects of FGFs and BMPs in chick mandibular morphogenesis. Dev Dyn 223:333-352.

Musella AE, Slater LJ. 1989. Familial florid osseous dysplasia: a case report. J Oral Maxillofac Surg 47:636-640.

Oetting WS, Mentink MM, Summers CG, Lewis RA, White JG, King RA. 1991. Three different frameshift mutations of the tyrosinase gene in type IA oculocutaneous albinism. Am J Hum Genet. 1991 Jul;49(1):199-206.

Oikarinen K, Altonen M, Happonen R-P. 1991. Gigantiform cementoma affecting a Caucasian family. Br J Oral Maxillofac Surg 29:194-197.

Park Y-K, Unni KK, McLeod RA, Pritchard DJ. 1993. Osteofibrous dysplasia: clinicopathologic study of 80 cases. Hum Pathol 24:1339-1347.

Patel MM, Wilkey JF, Abdelsayed R, D'Silva NJ, Malchoff C, Mallya SM. 2010. Analysis of GNAS mutations in cemento-ossifying fibromas and cemento-osseous dysplasias of the jaws. Oral Surg Oral Med Oral Pathol 109:739-743.

Petryk A, Anderson R, Jarcho MP, Leaf H, Carlson CS, Klingensmith J, Shawlot W, O'Connor MB. 2004. The mammalian twisted gastrulation gene functions in foregut and craniofacial development. Developmental Biology 267:374-386.

Pierce AM, Wilson DF, Goss AN. 1985. Inherited craniofacial fibrous dysplasia. Oral Surg Oral Med Oral Pathol 60:403-409.

Pierce AM, Sampson WJ, Wilson DF, Goss AN. 1996. Fifteen-year follow-up of a family with inherited craniofacial fibrous dysplasia. J Oral Maxillofac Surg 54:780-788.

Reitzik M, Lownie JF. 1975. Familial polyostotic fibrous dysplasia. Oral Surg Oral Med Oral Pathol 40:769-774.

Riminucci M, Saggio I, Gehron-Robey P, Bianco P. 2007. Fibrous dysplasia as a stem cell disease. J Bone Miner Res 21:P125-P131.

Rosen IB, Palmer JA. 1981. Fibroosseous tumors of the facial skeleton in association with primary hyperparathyroidism: an endocrine syndrome or coincidence? Am J Surg 142:494-498.

Ross JJ, Shimmi O, Vilmos P, Petryk A, Kim H, Gaudenz K, Hermanson S, Ekker SC, O'Connor MB, Marsh JL. 2001. Twisted gastrulation is a conserved extracellular BMP antagonist. Nature 410:479-483.

Sakamoto A, Oda Y, Iwamoto Y, Tsuneyoshi M. 2000. A comparative study of fibrous dysplasia and osteofibrous dysplasia with regard to Gs alpha mutation at the Arg201 codon: polymerase chain reaction-restriction fragment length polymorphism analysis of paraffin-embedded tissues. J Mol Diagn 2:67-72.

Sarkar AK, Gosh AK, Chowdhury SN, Biswas SK, Bag SK. 1993. Indian J Pediatr 60:301-305.

Scott IC, Blitz IL, Pappano WN, Maas SA, Cho KW, Greenspan DS. 2001. Homologues of Twisted gastrulation are extracellular cofactors in antagonism of BMP signalling. Nature 410:475-478.

Sedano HO, Kuba R, Gorlin RJ. 1982. Autosomal dominant cemental dysplasia. Oral Surg Oral Med Oral Pathol Oral Radiol Endod 54:642-646.

Shore EM, Xu M, Feldman GJ, Fenstermacher DA, Cho TJ, Choi IH, Connor JM, Delai P, Glaser DL, LeMerrer M, Morhart R, Rogers JG, Smith R, Triffitt JT, Urtizberea JA, Zasloff M, Brown MA, Kaplan FS. 2006. A recurrent mutation in the BMP type I receptor ACVR1 causes inherited and sporadic fibrodysplasia ossificans progressiva. Nat Genet 38:525-527.

Slaney SF, Goodman FR, Eilers-Walsman BL, Hall BD, Williams DK, Young ID, Hayward RD, Jones BM, Christianson AL, Winter RM. 1999. Acromelic frontonasal dysostosis. Am J Med Genet 83:109-16.

Smith JD, Hing AV, Clarke CM, Johnson NM, Perez FA, Park SS, Horst JA, Mecham B, Maves L, Nickerson DA; University of Washington Center for Mendelian Genomics, Cunningham ML. 2014.
Exome sequencing identifies a recurrent de novo *ZSWIM6* mutation associated with acromelic frontonasal dysostosis. Am J Hum Genet. 2014 Aug 7;95(2):235-4.

Sotillo Rodriguez, J. E., Mansky, K. C., Jensen, E. D., Carlson, A. E., Schwarz, T., Pham, L., MacKenzie, B., Prasad, H., Rohrer, M. D., Petryk, A. Gopalakrishnan R. 2009. Enhanced osteoclastogenesis causes osteopenia in twisted gastrulation-deficient mice through increased BMP signaling. J Bone Miner Res 24:1917-1926.

Stottmann RW, Anderson RM, Klingensmith J. 2001. The BMP antagonists Chordin and Noggin have essential but redundant roles in mouse mandibular outgrowth. Dev Biol 240:457-473.

Talley DB (with comment of Dr. Lester Cahn). 1952. Familial fibrous dysplasia of the jaws. Oral Surg Oral Med Oral Pathol 5:1012-1019.

Thakkar NS, Horner K, Sloan P. 1993. Familial occurrence of periapical cemental dysplasia. Virchows Arch A Pathol Anat Histopathol 423:233-236.

Toyosawa S, Yuki M, Kishino M, Ogawa Y, Ueda T, Murakami S, Konishi E, Iida S, Kogo M, Komori T, Tomita Y. 2007. Ossifying fibroma vs fibrous dysplasia of the jaw: molecular and immunological characterization. Mod Pathol 20:389-396.

Vainio S, Karavanova I, Jowett A, Thesleff I. 1993. Identification of BMP-4 as a signal mediating secondary induction between epithelial and mesenchymal tissues during early tooth development. Cell 75:45-58.

Van Hateren N., Shenton T., and Borycki A-G. 2006. Expression of Avian C-Terminal Binding Proteins (Ctbp1 and Ctbp2) During Embryonic Development. DEVELOPMENTAL DYNAMICS 235:490–495.

Weinstein LS, Shenker A, Gejman PV, Merino MJ, Friedman E, Spiegel AM. 1991. Activating mutations of the stimulatory G protein in the McCune-Albright syndrome. N Engl J Med 325:1688-1695.

Young SK, Markowitz NR, Sullivan S, Seale TW, Hirschi R. 1989. Familial gigantiform cementoma: classification and presentation of a large pedigree. Oral Surg Oral Med Oral Pathol 68:740-747.

Zhang P, Liégeois NJ, Wong C, Finegold M, Hou H, Thompson JC, Silverman A, Harper JW, DePinho RA, Elledge SJ. 1997. Altered cell differentiation and proliferation in mice lacking p57KIP2 indicates a role in Beckwith-Wiedemann syndrome. Nature. 1997 May 8;387(6629):151-8.

Zohar Y, Grausbord R, Shabtai F, Talmi Y. 1989. Fibrous dysplasia and cherubism as an hereditary familial disease. J Craniomaxillofac Surg 17:340-344.